A novel Rho-mDia2-HDAC6 pathway controls podosome patterning through microtubule acetylation in osteoclasts

Olivier Destaing[1,*,‡], Frédéric Saltel[1,*,§], Benoit Gilquin[2], Anne Chabadel[1], Saadi Khochbin[2], Stéphane Ory[3,*] and Pierre Jurdic[1,*,¶]

[1]Laboratoire de Biologie Moléculaire et Cellulaire, UMR 5665 CNRS/ENS, INRA 913, Ecole Normale Supérieure de Lyon, 46, allée d'Italie, 69364 Lyon CEDEX 7, France
[2]Laboratoire de Biologie Moléculaire et Cellulaire de la Différenciation, INSERM U309, Institut Albert Bonniot, Faculté de Médecine, 38706 La Tronche Cedex, France
[3]CRBM, CNRS FRE2593, 1919 route de Mende, 34293 Montpellier CEDEX 5, France
*These authors contributed equally to this work
‡Present address: Boyer Center for Molecular Medicine, Yale School of Medicine, 295 Congress Avenue, 06510 New Haven CT, USA
§Present address: CMU-Dpt physiologie cellulaire et métabolisme, 1 rue Michel Servet, 1211 Geneve 4, Switzerland
¶Author for correspondence (e-mail: pjurdic@ens-lyon.fr)

Accepted 6 April 2005
Journal of Cell Science 118, 2901-2911 Published by The Company of Biologists 2005
doi:10.1242/jcs.02425

Summary

Osteoclast maturation is accompanied by changes in podosome patterning, resulting in the formation of a peripheral belt, which requires an intact microtubule network. Here, we report that by inhibiting Rho, the podosome belt is maintained at the cell periphery despite depolymerisation of microtubules by nocodazole. Rho inhibition was correlated to the increase in microtubule stabilisation and microtubule acetylation. By microinjecting activated Rho or its activated effector mDia2 in osteoclasts, we found that the podosome belt was disrupted and the level of microtubule acetylation dramatically decreased. We further characterised the molecular mechanism responsible for microtubule deacetylation by co-immunoprecipitation experiments. We found that not only was mDia2 coprecipitating with the recently identified microtubule deacetylase HDAC6 but that it also activated the microtubule deacetylase activity of HDAC6 in an in vitro deacetylase assay. Finally, we found that during osteoclastogenesis, there is a correlation between the increase in microtubule acetylation and the podosome belt stabilisation and that if Rho is inhibited in the early stages of osteoclast differentiation, it accelerates both microtubule acetylation and podosome belt stabilisation. Altogether, our data reveal a pathway in which Rho interferes with the osteoclast maturation process by controlling the level of microtubule acetylation and actin organisation through mDIA2 and HDAC6.

Key words: HDAC6, Rho GTPase, mDIA, Microtubule acetylation, Podosomes, Osteoclasts

Introduction

By degrading mineralised matrix, multinucleated osteoclasts are crucial for the regulation of bone and calcium homeostasis. In the presence of M-CSF and RANK-L, monocyte-macrophage precursors fuse together to form large multinucleated cells in vitro (Boyle et al., 2003). Unlike most non-transformed cells, cells from monocytic lineage, including dendritic cells, macrophages and osteoclasts rely on podosomes to migrate or adhere to a substrate rather than on F-actin stress fibres or focal adhesion plaques. Podosomes are adhesion structures containing a column of a continuous flux of F-actin surrounded by focal adhesion proteins. In many respects, podosomes are similar to focal adhesion plaques as they are short-lived structures involved in cell migration, and share major focal adhesion proteins such as integrin, vinculin and talin as well as the signalling protein FAK/Pyk2 (for a review see Linder and Aepfelbacher, 2003). An important feature of podosomes is that they are associated with extracellular matrix degradation; they are thought to actively contribute to tissue invasion and matrix remodelling. For example, podosome clusters are found in highly motile and immature dendritic cells but not in static and mature cells found in tissues (Burns et al., 2001). These observations underscore the requirement of podosomes for cell migration. In vitro, osteoclast podosomes acquire a higher degree of self-organisation through the process of maturation. Immature osteoclasts exhibit clustered podosomes that are subsequently arranged into dynamic short-lived rings. Then, these podosome rings expand to the cell periphery to form a stable podosome belt in mature osteoclasts (Destaing et al., 2003). This podosome belt is reminiscent of the sealing zone found in resorbing osteoclasts, which provides tight attachment to bone and seals off the resorption pit where proteases and protons are secreted to degrade the bone matrix (Vaananen et al., 2000). The molecular mechanisms driving the transition from podosome clusters or dynamic rings to the podosome belt are presently unknown. However, recent evidence indicates that, as in focal adhesions and the formation of F-actin structures, microtubules and Rho GTPases are critical for podosome

patterning and assembly (for reviews, see Etienne-Manneville and Hall, 2002; Linder and Aepfelbacher, 2003). Similar to focal adhesions, microtubule plus ends may target podosomes (Kaverina et al., 1999; Evans et al., 2003) and microtubule network integrity has been shown to be crucial for podosome patterning (Destaing et al., 2003). Forced depolymerisation of microtubules by nocodazole treatment leads to the destabilisation of isolated podosomes in macrophages or in macrophage polykaryons (Linder et al., 2000; Ory et al., 2002) and, in osteoclasts, the podosome belt is disrupted. However, in the absence of polymerised microtubules and in contrast to macrophages, isolated podosomes are still formed in osteoclasts, indicating that in these cells, depolymerisation disrupts podosome patterning rather than the formation of podosomes themselves (Destaing et al., 2003).

Rho GTPases are known to promote F-actin and adhesion structure rearrangements and appear to be the probable signalling intermediates between microtubules and F-actin (Etienne-Manneville and Hall, 2003). Microtubule depolymerisation in fibroblasts promotes stress fibre formation and focal adhesion plaque assembly, which relies on RhoA activation (Enomoto, 1996; Ren et al., 1999). Although the function of Rho GTPases in podosome assembly or patterning is rather unclear, Rho GTPase activity needs to be tightly regulated to maintain podosome assembly (Linder and Aepfelbacher, 2003) and as in fibroblasts, microtubule dynamics regulates Rho GTPase activity (Ory et al., 2002). We recently showed that microtubule repolymerisation recapitulates the sequence of events that lead to podosome belt formation during osteoclast maturation. This process starts with podosome clustering at the early stage of microtubule repolymerisation and proceeds to the formation of podosome rings that eventually fuse together to generate the podosome belt at the cell periphery when microtubules are fully regrown (Destaing et al., 2003). It should be noted that the kinetics of microtubule repolymerisation are faster than the reformation of the podosome belt, indicating that not only the dynamics of microtubules are crucial for early events in podosome patterning (clusters or rings) but also that the microtubule network needs to be in place or stabilised before the podosome belt can be formed. In cells, there are two pools of dynamic microtubules, those that exhibit dynamic instability and have half-lives of 5-10 minutes, and stabilised microtubules, which do not exhibit dynamic instability and persist for hours (Saxton et al., 1984; Schulze and Kirschner, 1986; Webster et al., 1987a; Webster et al., 1987b). Stable microtubules accumulate post-translational modifications including detyrosination or acetylation, and may contribute to specialised functions in cells (Bulinski and Gundersen, 1991; Palazzo et al., 2001b; Rosenbaum, 2000).

Starting with these observations, we decided to investigate the molecular mechanisms that drive microtubule-dependent podosome belt stabilisation in osteoclasts and the extent to which Rho GTPase is involved in this process. Here, we report that Rho inhibition prevents podosome belt disruption following microtubule depolymerisation by nocodazole and, more surprisingly, that Rho inhibition increases the resistance of microtubules to nocodazole. Checking for microtubule post-translational modifications, we found that stable microtubules were acetylated and not detyrosinated. This led us to investigate whether Rho was involved in microtubule acetylation in osteoclasts. We used the fact that the histone acetylase HDAC6 has recently been described as a microtubule deacetylase (Hubbert et al., 2002; Matsuyama et al., 2002) and that the Rho effectors of the mDia family are involved in the control of post-translational modification of microtubules (Palazzo et al., 2001b) as well as the coordination of the microtubule and actin networks (Watanabe et al., 1999). This allowed us to reveal a pathway where activation of Rho promotes the deacetylation of microtubules through mDia2 and HDAC6 activation. Moreover, we present evidence that the level of microtubule acetylation is important for osteoclast function.

Materials and Methods

Reagents

Nocodazole, trichostatin A (TSA) and n-butyrate (Sigma-Aldrich) were used at 2 μM, 3 μM and 5 μM. Human M-CSF and recombinant human RANK-L were produced as previously described (Destaing et al., 2003). Supernatants were used at a final dilution of 1% corresponding to about 20 ng/ml and 30 ng/ml recombinant M-CSF and RANK-L, respectively. Monoclonal antibody AC40 anti-actin, anti-β-tubulin (clone DM1A) and anti-acetylated tubulin monoclonal antibody 6-11B-1 were from Sigma; anti-β-tubulin (clone N357) from Amersham Life Science, anti-HA (clone Y11) from Santa Cruz Biotechnology and anti-GFP monoclonal antibody was from Roche and Clontech. Anti-detyrosinated tubulin was a kind gift from Didier Job (CEA, Grenoble, France) and anti-HDAC6 polyclonal was raised against C-terminal peptide (Seigneurin-Berny et al., 2001). F-actin distribution was revealed after incubation with TRITC-conjugated phalloidin (Molecular Probes). Coverslips were mounted in Prolong® Antifade (Molecular Probes). Apatite collagen complexes (ACCs) were prepared using a method described previously (Shibutani et al., 2000; Saltel et al., 2004).

Plasmids and constructs

GFP-mDIA2 and GFP-mDIA2-ΔGBD were from Art Alberts (Van Andel Institute) and have been described previously (Palazzo et al., 2001a). GFP-G14VRho and GFP-G12VRac were gifts from Philippe Fort (CRBM, Montpellier, France). pEGFP-Actin Vector® was from Clontech. TAT-C3 expression vector was a kind gift from Erik Sahai and was produced as described (Coleman et al., 2001). Vectors expressing haemagglutinin (HA)-tagged mHDAC6 and deletion mutants have been described previously (Seigneurin-Berny et al., 2001).

Osteoclast differentiation

Spleen cells from six- to eight-week-old male OF1 mice were seeded at 2500 cells/mm^2 and cultured for 8 days on coverslips in differentiation medium: α-MEM medium (Life Technologies) containing 10% foetal calf serum (FCS, Hyclone) plus M-CSF and soluble recombinant RANK-L.

Microinjection

Mouse spleen cell-derived osteoclasts differentiated in vitro on Eppendorf CELLocate® coverslips for 7 days in differentiation medium were transferred to observation medium: α-MEM without bicarbonate (Life Technologies) containing 10% foetal calf serum, M-CSF, 20 mM HEPES and soluble recombinant RANK-L. Intranuclear microinjections of cDNA (0.2 mg/ml in 0.05 M Tris-HCl, pH 7.4) were carried out at room temperature using Eclipse TE 200 inverted microscope (Nikon) with an InjectMan micromanipulator and an Eppendorf 5246 microinjector. After injection, cells were further

maintained at 37°C and 5% CO_2 for 6 hours in differentiation medium before imaging.

Immunoprecipitation and interaction site mapping

For co-immunoprecipitation and interaction site mapping, COS cells were lysed 24 hours after transfection with Fugene 6® following the manufacturer's recommendations (Roche). Lysis buffer consists of 100 mM HEPES pH 7.9, 6 mM $MgCl_2$, 40% glycerol, 150 mM KCl, 0.1% Nonidet P40 and 1 mM dithiothreitol supplemented with a protease inhibitor cocktail. The lysate was incubated on ice for 20 minutes and cleared by centrifugation at 17,000 ***g*** for 10 minutes at 4°C. HA-tagged proteins were immunoprecipitated with anti-HA antibody and protein-G sepharose for 2 hours at 4°C. Immunoprecipitated proteins were washed three times in lysis buffer.

Confocal microscopy

For immunofluorescence, cells were fixed in Busson fixation solution at pH 6.9 (4% paraformaldehyde, 60 mM PIPES, 25 mM HEPES, 20 mM EGTA, 2 mM magnesium acetate, 0.05% glutaraldehyde w/v), processed as described (Ory et al., 2000) and imaged with a Zeiss LSM 510 microscope using a 63× (NA 1.4) Plan NeoFluor objective. To prevent cross-contamination between fluorochromes, each channel was imaged sequentially using the multi-track recording module before merging.

Tubulin deacetylase assay

COS cells transfected with 1 μg HDAC6 and/or mDia plasmids were lysed at room temperature for 40 minutes in buffer A (15 mM Tris-HCl, pH 7.4, 15 mM NaCl, 60 mM KCl, 340 mM sucrose, 2 mM EDTA, 0.5 mM EGTA, 0.65 mM spermidine, 1 mM dithiothreitol, 0.5% Triton X-100, 50 ng/ml TSA) with a complete protease inhibitor cocktail (Roche Molecular Biochemicals). After centrifugation at 17,000 ***g*** at 4°C, the supernatant (cytoplasmic extract) was mixed with Laemmli buffer and the extent of tubulin acetylation monitored by western blotting, using an anti-acetylated tubulin antibody.

GTP-GTPase affinity precipitation assay

The GST-RBD construct used to evaluate the level of GTP-Rho in cell lysates was kindly provided by M. Schwartz (Scripps Research Institute, La Jolla, CA). The activity assay was performed as described (Ren et al., 1999) for GTP-Rho with slight modifications. Briefly, GST-fusion proteins containing the Rho-binding domain (RBD) from mouse Rhotekin (amino acids 7-89) were produced in *Escherichia coli* BL21 cells. After isopropylthiogalactoside (IPTG) induction, pellets of bacteria were resuspended in lysis buffer (50 mM Tris-HCl, pH 8, 2 mM $MgCl_2$, 0.2 mM $Na_2S_2O_5$, 10% glycerol, 20% sucrose, 2 mM DTT, 1 μg/ml each aprotinin, leupeptin and pepstatin) and sonicated. Cell lysates were centrifuged for 20 minutes at 4°C, 45,000 ***g*** and the supernatants were incubated with glutathione-coupled sepharose 4B beads (Pharmacia Biotech) for 2 hours at 4°C. After three washes with lysis buffer, the amount of GST-RBD fusion proteins bound to the beads was estimated from Coomassie Blue-stained SDS gels.

Cells at different stages of the differentiation process were rapidly washed in ice-cold PBS and proteins were extracted with lysis buffer (50 mM Tris-HCl, pH 7.4, 5 mM $MgCl_2$, 1% Triton-X100, 10% glycerol, 0.5% sodium deoxycholate, 0.1% SDS, 500 mM NaCl and 1 μg/ml each leupeptin, pepstatin and aprotinin). Lysates were centrifuged for 5 minutes at 17,000 ***g*** and 4°C, and aliquots from the supernatant were used to determine total GTPase in the cell lysate. 20 μg of bacterially produced GST, GST-RBD fusion proteins bound to glutathione-coupled sepharose beads were added to cell lysates and incubated for 1 hour at 4°C. Beads were washed four times in lysis buffer and bound proteins were eluted in Laemmli sample buffer. Analyses for bound GTPases by western blotting were performed using monoclonal antibody 26C4 against RhoA (a generous gift from J. Bertoglio, Inserm U461, Paris, France).

Results

Rho inhibition slows down podosome belt disruption following microtubule depolymerisation

As microtubule integrity is required for podosome belt formation in mature osteoclasts (Destaing et al., 2003) and the small GTPase Rho is activated by microtubule depolymerisation in fibroblasts (Ren et al., 1999) or in macrophage osteoclast-like polykaryons (Ory et al., 2002), we wondered whether podosome belt destabilisation after microtubule depolymerisation was dependent on Rho activity. To address that question, we used the ability of exoenzyme C3 fused to the HIV TAT protein fragment (TAT-C3) to inhibit Rho activity quickly (Coleman et al., 2001; Nagahara et al., 1998; Schwarze et al., 1999). We first verified, using an in vitro ribosylation assay, that TAT-C3 efficiently inhibited Rho after 5 hours in osteoclasts (data not shown). Then, to examine the requirement of Rho activity for podosome belt destabilisation after microtubule depolymerisation, we maintained the osteoclasts for 5 hours in medium containing either TAT-C3, or TAT-GFP fusion proteins as a control, and treated them with nocodazole for 0, 30, 60 or 90 minutes. The cells were then fixed and stained for actin and β-tubulin (Fig. 1A). TAT-C3 alone neither affected the podosome belt nor the microtubule network (Fig. 1B). However, whereas the podosome belt started to be disassembled into podosome clusters after 30 minutes of nocodazole treatment, (Fig. 1A,B arrowheads), it remained tightly associated at the cell periphery in TAT-C3 treated osteoclasts (Fig. 1B). Longer treatment with nocodazole led to complete disruption of the podosome belt followed by cell retraction in control cells, whereas C3 treatment drastically delayed podosome belt disassembly as even after 90 minutes nocodazole treatment, the podosome belt was maintained at the cell periphery (Fig. 1A). This

Table 1. Percentage of osteoclasts presenting podosome belts compared to podosomes arranged in clusters or rings after various treatments*

	Control	Nocodazole (50 minutes)	TAT-C3 (5 hours)	TAT-C3 (5 hours) then nocodazole (50 minutes)	TAT-GFP (5 hours)	TAT-GFP (5 hours) then nocodazole (50 minutes)
% of cells with podosome rings	27	90	15	35	22	95
% of cells with podosome belts	73	10	85	65	78	5

*600 osteoclasts were counted for each condition and the results are from five independent experiments.

observation that TAT-C3 treatment prevented podosome belt disruption following depolymerisation of microtubules was further confirmed by quantifying the relative amount of osteoclasts with podosome belts compared to rings (Table 1). Longer nocodazole treatment resulted in the total loss of the podosome belt under both conditions, confirming the crucial role of microtubules in podosome belt integrity (data not shown).

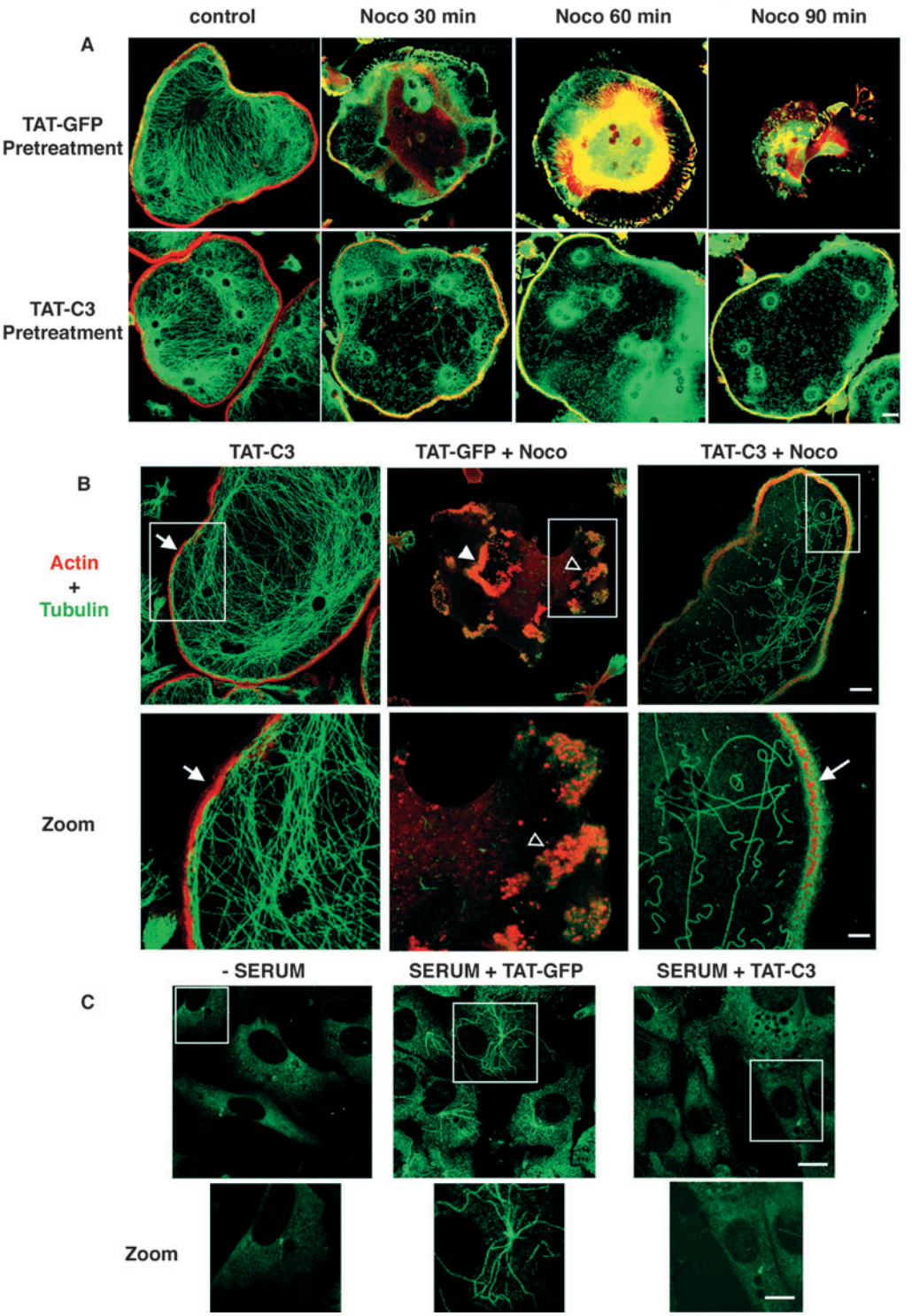

Fig. 1. TAT-C3-mediated Rho inhibition in osteoclasts confers podosome belt resistance to microtubule depolymerisation through stabilisation of a subset of microtubules. Rho-inhibition partially blocks nocodazole-induced microtubule depolymerisation and podosome belt dissociation. Osteoclasts either untreated or treated for 5 hours in the presence of TAT-GFP (0.5 μM) or TAT-C3 (0.5 μM) were incubated in the presence of nocodazole (2 μM) for 50 minutes and then fixed and stained for actin (in red) and β-tubulin (in green) before observation using a confocal microscope. (A) Kinetics of nocodazole-mediated podosome belts and microtubule disruption. In the presence of the control (TAT-GFP), nocodazole disrupted both microtubules and podosome belts in less than 30 minutes. In the presence of TAT-C3, podosomes belts were resistant to nocodazole treatment for more than 1 hour whereas subsets of microtubules were still observed. (B) TAT-C3 pretreatment had no effect on osteoclast cytoskeletons exhibiting a dense microtubule network and a podosome belt, whereas nocodazole induced complete microtubule dissociation together with podosome belt destabilisation and the subsequent formation of podosome rings (arrowheads) and clusters (open arrowheads) as previously described (Destaing et al., 2003). In contrast, TAT-C3 blocked the action of nocodazole since podosome belts were stabilised at the osteoclast periphery (arrows) and a subset of microtubules was maintained. A close-up of the area within the white insert is presented underneath each image. (C) Rho activation induces microtubule stabilisation in nocodazole-treated NIH3T3 cells. NIH3T3 cells were serum starved for 12 hours in the presence of TAT-GFP or TAT-C3 (0.5 μM) for the last 4 hours. Then cells were stimulated by serum addition for a further 2 hours before a 50-minute nocodazole (2 μM) treatment. Nocodazole-resistant microtubules were barely detectable when Rho was inactivated either in the absence of serum or in the presence of TAT-C3. In contrast, Rho activation by serum induced microtubule stabilisation in TAT-GFP control cells. A close-up of the area within the white insert is presented underneath each image. Bar, 10 μm (A, lower panels in B, C); 20 μm (upper panels in B).

Surprisingly, TAT-C3-treated osteoclasts showed a significant increase in nocodazole-resistant microtubules compared to TAT-GFP-treated cells (Fig. 1A,B). This observation contradicts previous published data showing that microtubule stabilisation is induced by Rho activation rather than Rho inhibition in NIH3T3 cells (Cook et al., 1998). To confirm that our results were not due to experimental deficiencies, we observed the microtubule content in NIH3T3 cells that were first stimulated by serum to activate Rho, and then treated with nocodazole in the presence of TAT-C3 or TAT-GFP. As described by others, and in contrast to osteoclasts, Rho activation by serum induced microtubule stabilisation that was otherwise blocked by TAT-C3 (Fig. 1C). We conclude that the effects of Rho inhibition on microtubule stability are cell type specific. It should be noted that microtubule stabilisation by Rho inhibition has also been found in astrocytes (S. Etienne-Manneville, personal communication).

Rho activity and HDAC6 regulate acetylated microtubule levels in osteoclasts

Our previous experiments indicating that Rho inhibition somehow stabilised microtubules prompted us to check whether the level of Rho activity could modulate post-translational modifications (PTMs) of microtubules, as PTMs are often associated with a change in microtubule dynamics and/or stability (Rosenbaum, 2000).

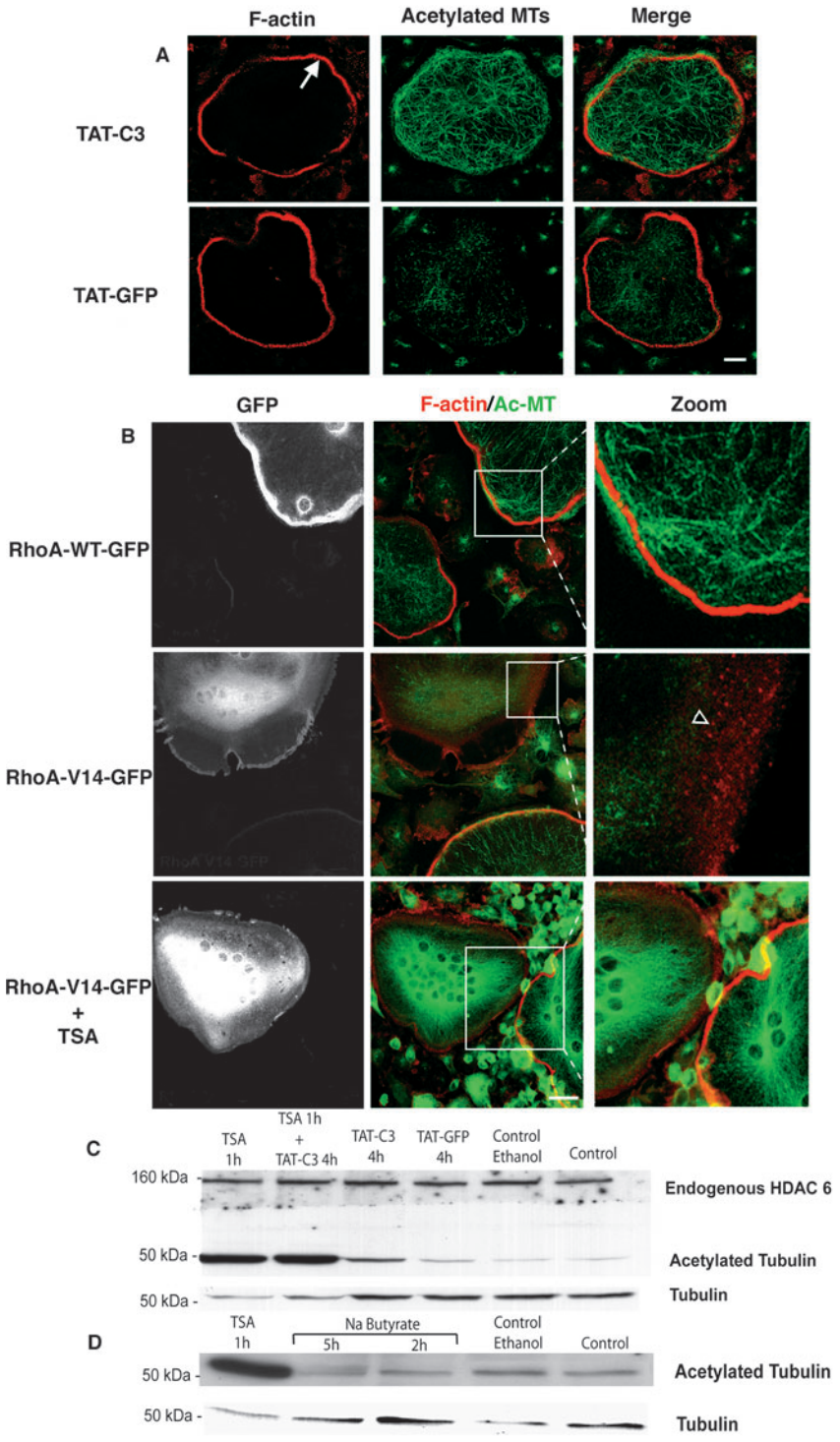

Fig. 2. Rho activity controls the level of tubulin acetylation upstream of HDAC6. (A) Inhibition of Rho by 0.5 μM TAT-C3 for 5 hours induced an accumulation of acetylated microtubules in comparison to 0.5 μM TAT-GFP used as a control. (B) One nucleus per osteoclast was microinjected with either RhoA WT-GFP or a constitutively activated form of Rho, RhoAV14-GFP expression vectors. Cells were fixed 6 hours after microinjection and GFP-expressing cells were detected by GFP fluorescence using a confocal microscope. Acetylated tubulin was detected by indirect immunofluorescence (green) and F-actin by means of phalloidin-RITC (red) and a close-up of each condition is presented. In the presence of RhoA-WT, osteoclasts exhibit the typical podosome belt and dense networks of acetylated microtubules. On the other hand, expression of Rho V14-GFP induced deacetylation of microtubules and disorganisation of podosome belts (arrowhead in close-up area). However, tubulin deacetylation dependent on Rho activation was inhibited after treatment with the HDAC6 inhibitor TSA (3 μM) for 1 hour, showing that this enzyme is downstream of Rho. (C,D) HDAC6 is present and active in osteoclasts. Endogenous HDAC6 was easily detected in osteoclasts by western blotting with a polyclonal anti-HDAC6 antibody (C). The deacetylase activity of HDAC6 was tested with two drugs: TSA, known to inhibit its activity and sodium butyrate, which does not. HDAC6 was indeed active in osteoclasts as confirmed by greatly increased levels of acetylated tubulin in TSA-treated osteoclasts and unchanged levels in the presence of sodium butyrate compared to the control and to the total amount of β-tubulin (D). Finally, inhibition of Rho by TAT-C3 (for 4 hours) in the presence of TSA had no additional effect on the increase in acetylated tubulin (C). Bar, 20 μm.

Osteoclasts were incubated for 5 hours with either TAT-GFP as a control or TAT-C3 to inhibit Rho, and processed for confocal microscopy analysis after staining of their actin and acetylated-microtubule (Ac-MT) cytoskeleton. Whereas the Ac-MT level was detectable but low in osteoclasts incubated with TAT-GFP fusion protein, it was increased in osteoclasts maintained in presence of TAT-C3 (Fig. 2A). On the other hand, we never observed changes in detyrosinated microtubules (data not shown), suggesting that Rho inhibition was promoting microtubule acetylation and also that Rho activation should trigger microtubule deacetylation. To test this hypothesis, one nucleus per osteoclast analysed was microinjected with vectors encoding GFP fused to a wild-type form or a constitutively activated form of RhoA (RhoA-WT, V14-RhoA respectively). Cells were then fixed and Ac-MT levels compared by immunostaining. GFP-RhoA WT did not significantly affect levels of Ac-MT whereas V14RhoA promoted a drastic decrease in the amount of Ac-MT together with disruption of the podosome belt (Fig. 2B). Thus, Rho appears to be a key player in regulating levels of Ac-MT in osteoclasts.

It has recently been shown that the histone deacetylase 6 (HDAC6) acts as a major microtubule deacetylase that can be inhibited by TSA (Matsuyama et al., 2002). To test whether HDAC6 could act on the Rho pathway, multinucleated osteoclasts were microinjected with V14RhoA cDNA and treated with TSA for 30 minutes. TSA treatment blocked the V14RhoA-mediated deacetylation of microtubules (Fig. 2B, lower panel), indicating that HDAC6 was downstream of Rho. To confirm that microtubule acetylation was increased by HDAC6 or Rho inhibition, we monitored levels of acetylated tubulin in osteoclast lysates treated with TAT-GFP, TAT-C3 or TSA (Fig. 2C). As expected, whereas levels of tubulin were comparable between samples, levels of acetylated tubulin increased an average of 2.5-fold in TAT-C3-treated osteoclasts when compared to TAT-GFP-treated osteoclasts (mean of five independent experiments). However, the relative increase of acetylated tubulin was much higher in TSA-treated compared to C3-treated cells indicating that Rho may partially control tubulin acetylation and/or only affect a subset of microtubules. In addition, in contrast to most HDAC proteins, TSA-sensitive HDAC6 has been shown to be insensitive to sodium butyrate. To assess whether microtubule deacetylation was dependent on other HDACs in osteoclasts, cells were treated with TSA or sodium butyrate and the amount of acetylated tubulin determined by western blotting. The amount of acetylated tubulin did not change in sodium butyrate-treated osteoclasts but did drastically increase when osteoclasts were treated with TSA (Fig. 2D). Altogether, these experiments indicate that Rho activation is able to stimulate microtubule deacetylation and that HDAC6 is a probable intermediate.

Rho activates HDAC6 via mDia2

To further evaluate the role of the Rho pathway in microtubule acetylation in osteoclasts, we decided to test whether the two best-characterised Rho effectors, namely ROCK and mDia proteins, modified levels of Ac-MT in osteoclasts. As the ROCK inhibitor Y27632 did not modify levels of Ac-MT in osteoclasts (data not shown), we focused on mDia2. Indeed, mDia2 was a good candidate as it has been shown to be involved in microtubule stabilisation and in coordinating microtubule and actin dynamics (Ishizaki et al., 2001; Palazzo et al., 2001a). We thus microinjected plasmids encoding a constitutive active mutant of mDia2 fused to GFP (GFP-mDIA2-ΔGBD) into osteoclasts (Palazzo et al., 2001a). Consistent with the effect of activated Rho, we found that activated mDia2 triggered a drastic decrease in levels of Ac-MT as well as disruption of the podosome belt without any new specific actin structures being formed (Fig. 3A). As our results suggest that both HDAC6 and mDia2 act downstream of Rho, we hypothesised that mDia2 and HDAC6 could interact together to regulate tubulin acetylation. To test this hypothesis, we cotransfected HDAC6 with either wild-type mDia2 or activated mDia2 fused to GFP (GFP-mDia2WT or GFP-mDIA2-ΔGBD) in COS cells. As a control, HDAC6 was transfected with GFP alone. HDAC6 proteins were then immunoprecipitated from cleared cell lysates and associated mDia2 revealed by immunoblotting with anti-GFP antibody. GFP-mDia2WT and GFP-mDIA2-ΔGBD were found in HDAC6 immunoprecipitates whereas GFP alone was not (Fig. 3B). To gain further insight into which HDAC6 domains were responsible for mDia2 binding, we cotransfected deletion mutants of HA-tagged HDAC6 together with GFP-mDia2WT. HDAC6 fragment proteins were immunoprecipitated with HA antibody and associated mDia2 was revealed by anti-GFP immunoblotting. We detected mDia2 in the DD1 (amino acids 85-428) and DD2 (aa 429-824) but not in the C-terminal (aa 825-1149) and N-terminal (aa 1-84) domain immunocomplexes (Fig. 3C). These results indicate that HDAC6 interacts with mDia2 in COS cells and that the two deacetylase domains, DD1 and DD2 are both able to interact with mDia2. Finally, to determine whether mDia2 was able to stimulate the deacetylase activity of HDAC6 in cells, we used an in vitro deacetylase assay (Zhang et al., 2003). COS cells were transfected with either HDAC6 alone, GFP-mDia2 alone or HDAC6 and GFP-mDia2 together. We then analysed the level of acetylated tubulin by western blotting of COS cell lysates (Fig. 3D). HDAC6 or GFP-mDia2 alone was not able to promote deacetylation of tubulin. However, when both proteins were expressed in cells, the level of acetylated tubulin was clearly reduced despite comparable amounts of tubulin in the samples. Moreover, transfecting twice the amount of GFP-mDia2 still reduced the level of acetylated tubulin indicating that mDia2 is able to activate HDAC6 deacetylase activity.

Formation of podosome belts in maturing osteoclasts correlates with microtubule acetylation

Our results described above clearly indicated that, in osteoclasts, Rho downregulation is required for podosome belt stabilisation, microtubule acetylation and stabilisation. We have previously reported that during in vitro osteoclastogenesis, podosome patterning evolves from microtubule-independent clusters and rings to microtubule-dependent belts (Destaing et al., 2003). We then reasoned that osteoclast maturation during osteoclastogenesis should be accompanied by an increase in microtubule acetylation. To investigate this possibility, we compared the Ac-MT pattern in macrophages, as well as in immature and mature osteoclasts seeded on glass. In macrophages, Ac-MT staining was concentrated in punctate structures resembling centrosomes (Fig. 4A). Immature osteoclasts exhibiting podosome rings

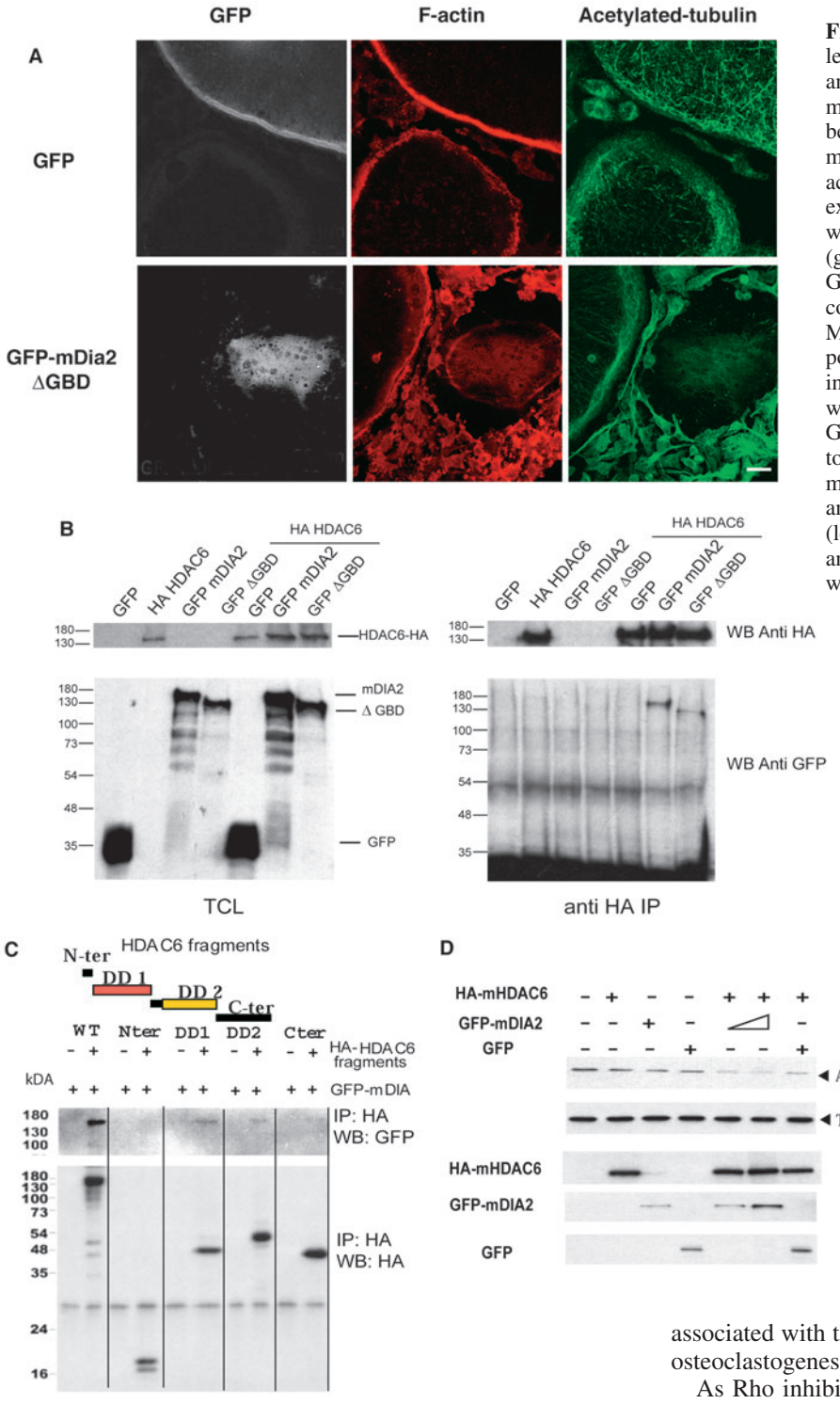

Fig. 3. mDIA2 mediates the action of Rho at the level of acetylated microtubules by interacting with and activating HDAC6. (A) Constitutively active mDia2 blocks tubulin acetylation and podosome belt formation. One nucleus per osteoclast was microinjected with either GFP or a constitutively activated form of mDIA2, GFP-mDIA2 ΔGBD expression vectors. 6 hours later, acetylated tubulin was detected by indirect immunofluorescence (green) and F-actin with phalloidin-RITC (red). In GFP-mDIA2 ΔGBD-expressing osteoclasts compared to GFP-expressing osteoclasts, the Ac-MT level was dramatically decreased and the podosome belt disrupted. (B) HDAC6 and mDia2 interact together. COS cells were either transfected with GFP alone, HA-HDAC6, GFP-mDIA2 WT, GFP-mDIA2 ΔGBD vectors or co-transfected together with HDAC6. Transfected HDAC6 or mDia2 were revealed in total cell lysate (TCL) by an anti-HA or an anti-GFP antibody respectively (left panel). HDAC6 was immunoprecipitated with an anti-HA antibody and mDia2-associated proteins were revealed with an anti-GFP antibody (right panel). Both the wild type and activated mDia2 co-precipitated with HA-tagged HDAC6. (C) Mapping of HDAC6 domain interaction with mDia2. To determine the domains of HDAC6 implicated in the interaction with GFP-mDIA2 WT, COS cells were transfected with GFP-mDIA2 WT and with the N-terminal domain, the deacetylase domain 1 (DD1), the deacetylase domain 2 (DD2) or the C-terminal domain of HDAC6, using HA-tagged expression vectors. Cell lysates of transfected cells were immunoprecipitated with a monoclonal anti-HA antibody. (D) mDia2 increases HDAC6 deacetylase activity. In a tubulin deacetylase in vitro assay, COS cells were transfected with mHDAC6-HA WT, lysed at room temperature for 15 minutes and the ratio of acetylated tubulin/tubulin monitored by western blotting. When GFP-mDIA2 WT was transfected with mHDAC6-HA WT, this increased the deacetylase activity of the enzyme whereas GFP-mDIA2 WT alone had no effect on the level of this PTM. Positions of protein standards in kDa are indicated on the left-hand side of blots.

contained only a low level of Ac-MT (Fig. 4B) whereas mature osteoclasts, with a podosome belt, had much higher levels of Ac-MT which were found mostly associated with the actin podosome belt (Fig. 4C, arrowhead). This was further assessed by comparing acetylated tubulin levels in cultures of osteoclasts after 6 or 8 days of differentiation containing 40% or 80% respectively, of osteoclasts exhibiting podosome belts (Fig. 4D). We could conclude that microtubule acetylation is associated with the formation of stable podosome belts during osteoclastogenesis.

As Rho inhibition is crucial for maintaining the podosome belt at the cell periphery, we expected that Rho inhibition in immature osteoclasts (D6) should accelerate the formation of podosome belts. Macrophages were differentiated into osteoclasts and at day 6, TAT-GFP or TAT-C3 was added to the differentiation medium for 6 hours. The number of osteoclasts with podosome rings (Fig. 4E, arrowhead) or podosome belts (Fig. 4E, arrows) was then quantified and compared to cells maintained in differentiation medium alone. At day 6, only 40% of osteoclasts in untreated or TAT-GFP-treated osteoclasts exhibited podosome belts versus 70% in TAT-C3-treated

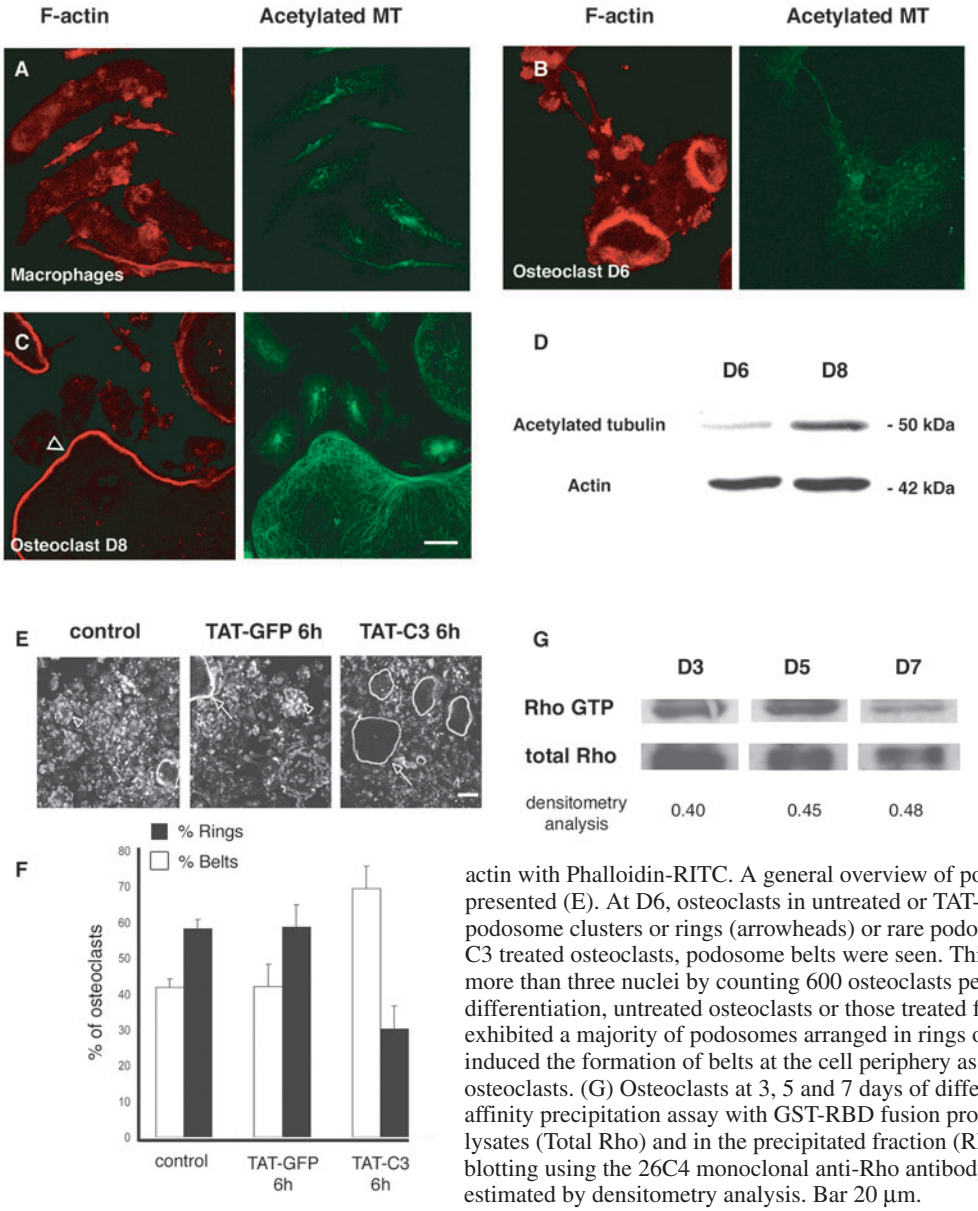

Fig. 4. The level of microtubule acetylation in mature osteoclasts correlates with stabilisation of podosomes into belts. (A,B) Macrophages and immature osteoclasts, differentiated for 6 days in the presence of RANK-L + M-CSF, with podosome rings, presented a low level of acetylated tubulin. (C) Mature osteoclasts differentiated for 8 days in the presence of RANK-L + M-CSF presented specific accumulations of acetylated microtubules just behind the podosome belt (arrowhead). (D) This specific accumulation of acetylated microtubules during the transition period between podosome rings and belt, the last step of podosome patterning, was confirmed by western blot analysis on osteoclast populations differentiated for 6 (D6) or 8 (D8) days. Standard protein markers are indicated in kDa. (E,F) Rho inhibition accelerates the podosome ring to belt transition in immature osteoclasts. Spleen leukocytes were differentiated in the presence of RANKL and M-CSF for 6 days, and then treated or not with TAT-GFP or TAT-C3 for 6 hours before being fixed, and stained for F-actin with Phalloidin-RITC. A general overview of podosome organisation in osteoclasts is presented (E). At D6, osteoclasts in untreated or TAT-GFP treated cultures exhibited mostly podosome clusters or rings (arrowheads) or rare podosome belt (arrows). In contrast, in TAT-C3 treated osteoclasts, podosome belts were seen. This was quantified in osteoclasts containing more than three nuclei by counting 600 osteoclasts per condition (F). At this stage of differentiation, untreated osteoclasts or those treated for 6 hours with TAT-GFP (0.5 μM) exhibited a majority of podosomes arranged in rings or clusters, whereas TAT-C3 (0.5 μM) induced the formation of belts at the cell periphery as usually found in more mature osteoclasts. (G) Osteoclasts at 3, 5 and 7 days of differentiation were lysed to perform an affinity precipitation assay with GST-RBD fusion proteins. The amount of Rho in total cell lysates (Total Rho) and in the precipitated fraction (RhoGTP) was determined by western blotting using the 26C4 monoclonal anti-Rho antibody. The ratio of RhoGTP/total Rho was estimated by densitometry analysis. Bar 20 μm.

osteoclasts (Fig. 4F). In an attempt to confirm the relation between the level of Rho activation, microtubule deacetylation and the podosome belt formation we performed GST-pull down experiments to evaluate the RhoGTP levels along osteoclastogenesis. Unfortunately, we could not detect any significant variation of the ratio of RhoGTP versus total Rho (Fig. 4G). This may indicate that the localisation of activated Rho is more important to mediate its effect than the overall Rho activity. Nevertheless, altogether our results in osteoclasts indicate that Rho is involved in podosome belt formation as well as in cytoskeleton maturation process by promoting a switch from podosome rings to podosome belts, although its precise mode of action remains to be elucidated.

Bone resorbing osteoclasts exhibit high levels of acetylated microtubules within the sealing zone

As microtubule acetylation is an essential process in osteoclast maturation, we reasoned that this could be important in osteoclast function, namely bone resorption. When resorbing bone, osteoclasts rearrange their actin cytoskeleton into a sealing zone, a large band of actin that delineates the resorption pit. We have recently shown that osteoclasts alternate between resorbing phases with a sealing zone and migrating phases without any specific actin structures (Saltel et al., 2004). To determine whether microtubule acetylation could be correlated with osteoclast function, we cultured osteoclasts on coverslips coated with an apatite/collagen matrix known to mimic the bone surface (Shibutani et al., 2000; Saltel et al., 2004). Ac-MTs and detyrosinated microtubules were analysed with F-actin by immunostaining and confocal microscopy. Ac-MTs were barely detectable in migrating osteoclasts (Fig. 5B), but increased drastically in resorbing osteoclasts (Fig. 5A). Interestingly, resorbing or non-resorbing osteoclasts did not show any accumulation of detyrosinated microtubules (Fig. 5A,B), suggesting that microtubule acetylation may reflect a

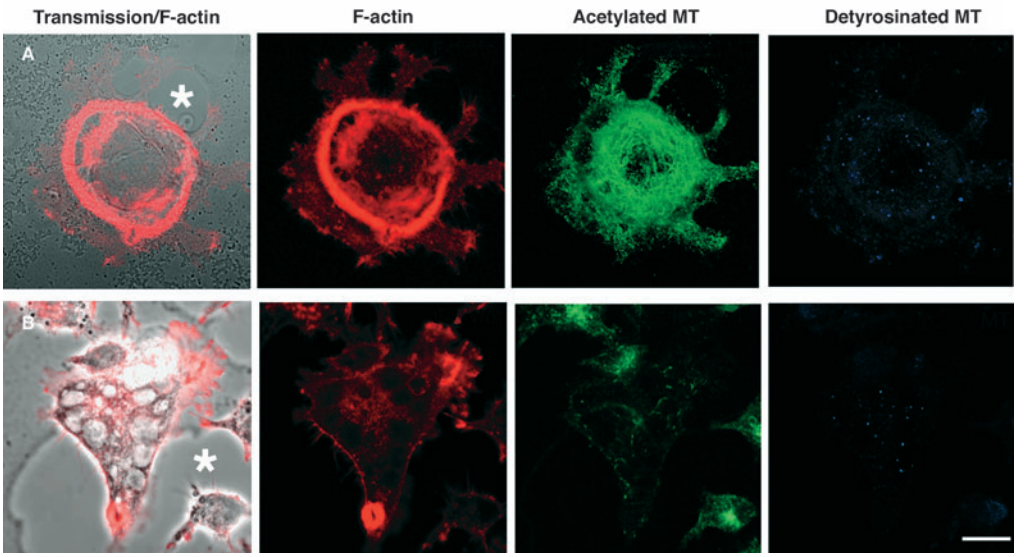

Fig. 5. Formation of the sealing zone in bone resorbing osteoclasts is associated with the dynamic regulations of tubulin acetylation. (A,B) Osteoclasts were differentiated in the presence of RANK-L + M-CSF for 8 days, detached, spread on mineralised matrix (ACC, Apatite Collagen Complex) substrate, which mimics dentin slices, fixed and immunostained with phalloidin-RITC and monoclonal anti-acetylated and polyclonal anti-detyrosinated tubulin antibodies. These two osteoclasts are associated with a resorption pit (*). The osteoclast presented in A is still resorbing, as it exhibits a sealing zone, a large band of F-actin, and has a large number of acetylated but undetectable detyrosinated microtubules. The osteoclast in B is a migrating osteoclast without a sealing zone and showed neither acetylated nor detyrosinated microtubules. Bar, 20 μm.

specific post-translational modification of microtubules in active osteoclasts.

Discussion

We previously reported that osteoclast differentiation was accompanied by a change in podosome patterning. Immature osteoclasts present dynamic podosome rings and mature osteoclasts contain a stable peripheral podosome belt (Destaing et al., 2003). In an attempt to understand the molecular mechanisms underlying podosome patterning, we found that Rho inhibition both delayed podosome belt disruption after nocodazole treatment and accelerated the switch from unstable podosome rings to a stable peripheral podosome belt, mimicking the maturation process. We also described for the first time that during the differentiation of osteoclasts and their resorption cycle on mineralised matrix, microtubules became acetylated, and not detyrosinated, indicating that microtubule acetylation may have a specific function in osteoclasts. Furthermore, stabilisation of the podosome belt was correlated with two events: increases in microtubule acetylation and Rho inhibition. This led us to identify a new Rho-dependent pathway in which the recently discovered microtubule acetylase HDAC6 (Hubbert et al., 2002; Matsuyama et al., 2002; Zhang et al., 2003) was activated by Rho and its effector mDia2. Microinjection of either activated RhoA or mDia2 triggered microtubule deacetylation together with podosome belt disruption. On the other hand, Rho inhibition promoted microtubule acetylation. In vitro assays confirmed that mDia2 activates the microtubule deacetylase activity of HDAC6 and this may be explained by the presence of HDAC6 and mDia2 in the same protein complex as revealed by immunoprecipitation experiments. Altogether, our results indicate that microtubule acetylation levels are controlled by Rho proteins, and that this may be crucial for osteoclast differentiation and function.

The fact that, in our study, TAT-C3-mediated Rho inhibition promoted podosome belt assembly during osteoclast maturation is rather surprising. Indeed, exoenzyme C3 has been reported to disrupt the sealing zone and to block osteoclast resorption on bone (Zhang et al., 1995; Saltel et al., 2004) as well as disrupting isolated podosomes in macrophage polykaryons (Chellaiah et al., 2000; Ory et al., 2000). In src-transformed cells, Rho inhibition also disrupted the podosome whereas activated Rho has been found localised in podosomes (Berdeaux et al., 2004). However, inconsistent with a function of Rho in podosome formation, and in contrast to Cdc42 (Dutartre et al., 1996; Moreau et al., 2003), activated Rho or, interestingly activated mDia, do not lead to typical podosome formation but rather to their disruption (Burgstaller and Gimona, 2004; Chellaiah et al., 2000; Ory et al., 2000) indicating that the Rho activation pathway by itself is not sufficient for podosome formation. However, as revealed by our recent study (Saltel et al., 2004), Rho inhibition in osteoclasts cultured on bone-like substrate led to the loss of both their resorptive function and their apico-basal polarity. Interestingly, under these conditions, F-actin reorganised into a podosome belt, mimicking the actin organisation found in osteoclasts seeded on glass, an organisation never seen in osteoclasts seeded on bone-like substrate in normal conditions. Together with the present study, it indicates that Rho activity is not required for the podosome belt formation. However, despite what we were expecting, we could not observe any RhoGTP level variation along osteoclastogenesis indicating that to get more insight into the function of Rho in such large multinucleated cells, the subcellular localisation of activated Rho should be investigated. It would be more informative than the overall activity measured by pull-down assay. Indeed, we should expect Rho to be only locally inhibited as its full inhibition by exoenzyme C3 triggered not only the podosome belt stabilisation, but also excessive spreading and loss of cell polarity (Ory et al., 2000; Saltel et al., 2004). This may engage local regulation of Rho activity, variations of which may be insufficient to discriminate it from the overall Rho activity in cells. This idea is also supported by the fact that acetylation of microtubules was mainly observed on a subset of microtubules localised in the vicinity of the podosome belt in differentiated

osteoclasts. This suggests that a local change in microtubule properties is occurring, and consequently, a local change in signalling events leading to microtubule acetylation.

Microtubule acetylation during osteoclast differentiation

Our results have shown that podosome belt and sealing zone formation during osteoclast maturation and bone resorption, respectively, are associated with an increase in tubulin acetylation corresponding to microtubule stabilisation. Interestingly, observations of increases in stable microtubules have been made in other differentiated cell types (Bulinski and Gundersen, 1991). For example, in muscle cell differentiation, which involves the fusion of myoblasts to form multinucleated myotubes, detyrosinated microtubules accumulate in myogenic precursors shortly before the fusion events. Detyrosinated microtubules are maintained in myotubes but acetylation is only observed at a later stage (Gundersen et al., 1989). Unlike myogenesis (Chang et al., 2002), osteoclastogenesis is not associated with detyrosination of microtubules, as we did not detect any significant changes in the levels of detyrosinated microtubules. However, as in myotubes, acetylated microtubules increased at a later stage in mature osteoclasts. These observations indicate that, although PTMs take place on stable microtubules, they are not necessarily occurring at the same time during the differentiation process, suggesting that they are dependent on their subcellular micro-environment and do not have the same biological functions. Differences in the function of post-translational tubulin modifications have been well exemplified in *Tetrahymena thermophila* in which the endogenous β-tubulin gene has been replaced by mutated forms preventing either acetylation or polyglycylation PTMs. Although there were no detectable abnormalities when non-acetylatable tubulin was expressed (Gaertig et al., 1995), preventing the polyglycylation of β-tubulin, in contrast, had an affect on cytokinesis and was lethal (Thazhath et al., 2002).

Although both the underlying molecular mechanisms of PTM and the function of microtubule acetylation remain to be elucidated, recent reports have highlighted an intriguing property of detyrosinated microtubules. In mammalian cells, kinesins have a stronger affinity for detyrosinated tubulin and may be preferentially recruited on stable detyrosinated microtubules (Gurland and Gundersen, 1995; Kreitzer et al., 1999). Whether a similar function can be attributed to acetylation remains to be seen, but microtubule acetylation is highly regulated in osteoclast resorption function and podosome patterning.

Rho activates HDAC6 through mDia2 and controls microtubule quality

HDAC6 has been recently characterised as a cytoplasmic tubulin deacetylase (Hubbert et al., 2002; Matsuyama et al., 2002; Zhang et al., 2003). We found that Rho inhibition increased microtubule acetylation. Conversely, Rho activation as well as microinjection of activated mDia2, promoted microtubule deacetylation whereas no changes in the levels of microtubule acetylation were observed with the ROCK inhibitor Y27632 (data not shown). These results indicate that mDia2 is the specific Rho effector involved in microtubule deacetylation. This hypothesis is reinforced by the fact that mDia2 coprecipitated with and activated HDAC6 in COS cells. Thus, we propose that Rho activates mDia2, which in turn stimulates HDAC6. However, the precise mechanism by which HDAC6 is activated will require more experiments. Indeed, we noticed that deacetylation of microtubules was not significantly different when HDAC6 was cotransfected with either the constitutively activated form of mDia2 (GFP-mDIA2-ΔGBD) or its wild-type counterpart. Together with the fact that mDia2 partially colocalised with HDAC6 on microtubules in osteoclasts (data not shown), we propose that an mDia2/HDAC6 complex is constitutively formed and that Rho activation localises that complex on microtubules to promote its in vivo deacetylation. Knowing where Rho is activated in this context is of major importance. Finally, mDia2 binding requires the cooperation of the deacetylase domains, DD1 and DD2 of HDAC6, which are also required for HDAC6 to bind tubulin (Zhang et al., 2003). Whether that complex is dependent upon tubulin binding to be assembled and/or active remains to be answered. Nonetheless, our results highlight the requirement for a fine control of Rho-dependent microtubule acetylation in osteoclasts. It would be of interest to analyse osteoclast podosome patterning in an HDAC6$^{-/-}$ background.

O.D. and F.S. are recipients of MENRT and FRM grants. We are grateful to Sandrine Etienne-Manneville for helpful discussions and sharing unpublished data. We wish to thank Art Alberts and Klaus Aktories for giving us precious reagents and also Jan R. De Mey and Edith Bonnely for stimulating discussions. B.G. is a recipient of a PhD fellowship from the Ligue Nationale Contre le Cancer, Comité de l'Isère. We are grateful to Sandrine Curtet-Benitski for technical assistance. This work was also supported by grants from CNRS (dynamique et réactivité du vivant), INSERM and the Ligue contre le Cancer du Rhône.

References

Berdeaux, R. L., Diaz, B., Kim, L. and Martin, G. S. (2004). Active Rho is localized to podosomes induced by oncogenic Src and is required for their assembly and function. *J. Cell Biol.* **166**, 317-323.

Boyle, W. J., Simonet, W. S. and Lacey, D. L. (2003). Osteoclast differentiation and activation. *Nature* **423**, 337-342.

Bulinski, J. C. and Gundersen, G. G. (1991). Stabilization of post-translational modification of microtubules during cellular morphogenesis. *BioEssays* **13**, 285-293.

Burgstaller, G. and Gimona, M. (2004). Actin cytoskeleton remodelling via local inhibition of contractility at discrete microdomains. *J. Cell Sci.* **117**, 223-231.

Burns, S., Thrasher, A. J., Blundell, M. P., Machesky, L. and Jones, G. E. (2001). Configuration of human dendritic cell cytoskeleton by Rho GTPases, the WAS protein, and differentiation. *Blood* **98**, 1142-1149.

Chang, W., Webster, D. R., Salam, A. A., Gruber, D., Prasad, A., Eiserich, J. P. and Bulinski, J. C. (2002). Alteration of the C-terminal amino acid of tubulin specifically inhibits myogenic differentiation. *J. Biol. Chem.* **277**, 30690-30698.

Chellaiah, M. A., Soga, N., Swanson, S., McAllister, S., Alvarez, U., Wang, D., Dowdy, S. F. and Hruska, K. A. (2000). Rho-A is critical for osteoclast podosome organization, motility, and bone resorption. *J. Biol. Chem.* **275**, 11993-12002.

Coleman, M. L., Sahai, E. A., Yeo, M., Bosch, M., Dewar, A. and Olson, M. F. (2001). Membrane blebbing during apoptosis results from caspase-mediated activation of ROCK I. *Nat. Cell Biol.* **3**, 339-345.

Cook, T. A., Nagasaki, T. and Gundersen, G. G. (1998). Rho guanosine triphosphatase mediates the selective stabilization of microtubules induced by lysophosphatidic acid. *J. Cell Biol.* **141**, 175-185.

Destaing, O., Saltel, F., Geminard, J. C., Jurdic, P. and Bard, F. (2003). Podosomes display actin turnover and dynamic self-organization in

osteoclasts expressing actin-green fluorescent protein. *Mol. Biol. Cell.* **14**, 407-416.

Dutartre, H., Davoust, J., Gorvel, J. P. and Chavrier, P. (1996). Cytokinesis arrest and redistribution of actin-cytoskeleton regulatory components in cells expressing the Rho GTPase CDC42Hs. *J. Cell Sci.* **109**, 367-377.

Enomoto, T. (1996). Microtubule disruption induces the formation of actin stress fibers and focal adhesions in cultured cells: possible involvement of the rho signal cascade. *Cell Struct. Funct.* **21**, 317-326.

Etienne-Manneville, S. and Hall, A. (2002). Rho GTPases in cell biology. *Nature* **420**, 629-635.

Etienne-Manneville, S. and Hall, A. (2003). Cdc42 regulates GSK-3beta and adenomatous polyposis coli to control cell polarity. *Nature* **421**, 753-756.

Evans, J. G., Correia, I., Krasavina, O., Watson, N. and Matsudaira, P. (2003). Macrophage podosomes assemble at the leading lamella by growth and fragmentation. *J. Cell Biol.* **161**, 697-705.

Gaertig, J., Cruz, M. A., Bowen, J., Gu, L., Pennock, D. G. and Gorovsky, M. A. (1995). Acetylation of lysine 40 in alpha-tubulin is not essential in Tetrahymena thermophila. *J. Cell Biol.* **129**, 1301-1310.

Gundersen, G. G., Khawaja, S. and Bulinski, J. C. (1989). Generation of a stable, posttranslationally modified microtubule array is an early event in myogenic differentiation. *J. Cell Biol.* **109**, 2275-2288.

Gurland, G. and Gundersen, G. G. (1995). Stable, detyrosinated microtubules function to localize vimentin intermediate filaments in fibroblasts. *J. Cell Biol.* **131**, 1275-1290.

Hubbert, C., Guardiola, A., Shao, R., Kawaguchi, Y., Ito, A., Nixon, A., Yoshida, M., Wang, X. F. and Yao, T. P. (2002). HDAC6 is a microtubule-associated deacetylase. *Nature* **417**, 455-458.

Ishizaki, T., Morishima, Y., Okamoto, M., Furuyashiki, T., Kato, T. and Narumiya, S. (2001). Coordination of microtubules and the actin cytoskeleton by the Rho effector mDia1. *Nat. Cell Biol.* **3**, 8-14.

Kaverina, I., Krylyshkina, O. and Small, J. V. (1999). Microtubule targeting of substrate contacts promotes their relaxation and dissociation. *J. Cell Biol.* **146**, 1033-1044.

Kreitzer, G., Liao, G. and Gundersen, G. G. (1999). Detyrosination of tubulin regulates the interaction of intermediate filaments with microtubules in vivo via a kinesin-dependent mechanism. *Mol. Biol. Cell.* **10**, 1105-1118.

Linder, S. and Aepfelbacher, M. (2003). Podosomes: adhesion hot-spots of invasive cells. *Trends Cell Biol.* **13**, 376-385.

Linder, S., Hufner, K., Wintergerst, U. and Aepfelbacher, M. (2000). Microtubule-dependent formation of podosomal adhesion structures in primary human macrophages. *J. Cell Sci.* **113**, 4165-4176.

Matsuyama, A., Shimazu, T., Sumida, Y., Saito, A., Yoshimatsu, Y., Seigneurin-Berny, D., Osada, H., Komatsu, Y., Nishino, N., Khochbin, S. et al. (2002). In vivo destabilization of dynamic microtubules by HDAC6-mediated deacetylation. *EMBO J.* **21**, 6820-6831.

Moreau, V., Tatin, F., Varon, C. and Genot, E (2003). Actin can reorganize into podosomes in aortic endothelial cells, a process controlled by Cdc42 and RhoA. *Mol. Cell Biol.* **23**, 6809-6822.

Nagahara, H., Vocero-Akbani, A. M., Snyder, E. L., Ho, A., Latham, D. G., Lissy, N. A., Becker-Hapak, M., Ezhevsky, S. A. and Dowdy, S. F. (1998). Transduction of full-length TAT fusion proteins into mammalian cells: TAT-p27Kip1 induces cell migration. *Nat. Med.* **4**, 1449-1452.

Ory, S., Munari-Silem, Y., Fort, P. and Jurdic, P. (2000). Rho and Rac exert antagonistic functions on spreading of macrophage-derived multinucleated cells and are not required for actin fiber formation. *J. Cell Sci.* **113**, 1177-1188.

Ory, S., Destaing, O. and Jurdic, P. (2002). Microtubule dynamics differentially regulates Rho and Rac activity and triggers Rho-independent stress fiber formation in macrophage polykaryons. *Eur. J. Cell Biol.* **81**, 351-362.

Palazzo, A. F., Cook, T. A., Alberts, A. S. and Gundersen, G. G. (2001a). mDia mediates Rho-regulated formation and orientation of stable microtubules. *Nat. Cell Biol.* **3**, 723-729.

Palazzo, A. F., Joseph, H. L., Chen, Y. J., Dujardin, D. L., Alberts, A. S., Pfister, K. K., Vallee, R. B. and Gundersen, G. G. (2001b). Cdc42, dynein, and dynactin regulate MTOC reorientation independent of Rho-regulated microtubule stabilization. *Curr. Biol.* **11**, 1536-1541.

Ren, X. D., Kiosses, W. B. and Schwartz, M. A. (1999). Regulation of the small GTP-binding protein Rho by cell adhesion and the cytoskeleton. *EMBO J.* **18**, 578-585.

Rosenbaum, J. (2000). Cytoskeleton: functions for tubulin modifications at last. *Curr. Biol.* **10**, R801-R803.

Saltel, F., Destaing, O., Bard, F., Eichert, D. and Jurdic, P. (2004). Apatite-mediated actin dynamics in resorbing osteoclasts. *Mol. Biol. Cell.* **15**, 5231-5241.

Saxton, W. M., Stemple, D. L., Leslie, R. J., Salmon, E. D., Zavortink, M. and McIntosh, J. R. (1984). Tubulin dynamics in cultured mammalian cells. *J. Cell Biol.* **99**, 2175-2186.

Schulze, E. and Kirschner, M. (1986). Microtubule dynamics in interphase cells. *J. Cell Biol.* **102**, 1020-1031.

Schwarze, S. R., Ho, A., Vocero-Akbani, A. and Dowdy, S. F. (1999). In vivo protein transduction: delivery of a biologically active protein into the mouse. *Science* **285**, 1569-1572.

Seigneurin-Berny, D., Verdel, A., Curtet, S., Lemercier, C., Garin, J., Rousseaux, S. and Khochbin, S. (2001). Identification of components of the murine histone deacetylase 6 complex: link between acetylation and ubiquitination signaling pathways. *Mol. Cell Biol.* **21**, 8035-8044.

Shibutani, T., Iwanaga, H., Imai, K., Kitago, M., Doi, Y. and Iwayama, Y. (2000). Use of glass slides coated with apatite-collagen complexes for measurement of osteoclastic resorption activity. *J. Biomed. Mater. Res.* **50**, 153-159.

Thazhath, R., Liu, C. and Gaertig, J. (2002). Polyglycylation domain of beta-tubulin maintains axonemal architecture and affects cytokinesis in Tetrahymena. *Nat. Cell Biol.* **4**, 256-259.

Vaananen, H. K., Zhao, H., Mulari, M. and Halleen, J. M. (2000). The cell biology of osteoclast function. *J. Cell Sci.* **113**, 377-381.

Webster, D. R., Gundersen, G. G., Bulinski, J. C. and Borisy, G. G. (1987a). Assembly and turnover of detyrosinated tubulin in vivo. *J. Cell Biol.* **105**, 265-276.

Webster, D. R., Gundersen, G. G., Bulinski, J. C. and Borisy, G. G. (1987b). Differential turnover of tyrosinated and detyrosinated microtubules. *Proc. Natl. Acad. Sci. USA* **84**, 9040-9044.

Zhang, D., Udagawa, N., Nakamura, I., Murakami, H., Saito, S., Yamasaki, K., Shibasaki, Y., Morii, N., Narumiya, S., Takahashi, N. et al. (1995). The small GTP-binding protein, rho p21, is involved in bone resorption by regulating cytoskeletal organization in osteoclasts. *J. Cell Sci.* **108**, 2285-2292.

Zhang, Y., Li, N., Caron, C., Matthias, G., Hess, D., Khochbin, S. and Matthias, P. (2003). HDAC-6 interacts with and deacetylates tubulin and microtubules in vivo. *EMBO J.* **22**, 1168-1179.